Transbilayer Transport of Ions and Lipids Coupled with Mastoparan X Translocation†

Katsumi Matsuzaki,* Shuji Yoneyama, Osamu Murase, and Koichiro Miyajima

Faculty of Pharmaceutical Sciences, Kyoto University, Sakyo-ku, Kyoto 606-01, Japan

Received February 12, 1996; Revised Manuscript Received April 22, 1996⊗

ABSTRACT: The transbilayer movement of ions and lipids induced by mastoparan X, a peptidic toxin from *Vespa xanthoptera*, was investigated by use of lipid vesicles as a model membrane system. Negatively charged phosphatidylglycerol remarkably enhanced the peptide−lipid interactions. Mastoparan X induced the ion flow by forming a short-lived, multimeric pore in the lipid bilayer, as determined from the leakage of an anionic dye, calcein, from the liposomes. The pore formation was coupled with the translocation of the peptide into the inner leaflet. The latter was detected by three experiments using fluorescence techniques [Matsuzaki, K., Murase, O., Fujii, N., & Miyajima, K. (1995) *Biochemistry 34*, 6521−6526; Matsuzaki, K., Murase, O., & Miyajima, K. (1995) *Biochemistry 34*, 12553−12559]. The lipid flip flop was monitored on the basis of the chemical quenching of 7-nitrobenz-2-oxa-1,3-diazol-4-yl (NBD)-labeled lipids by sodium dithionite. Mastoparan X triggered the rapid flip-flop of both negatively charged and zwitterionic lipids in coupling with the pore formation and the peptide translocation. A novel model of the mastoparan−lipid interactions was proposed to explain these observations.

Mastoparans are a class of peptidic toxins isolated from wasp venom, exhibiting various biological activities. They stimulate various secretory functions, e.g., histamine from mast cells (Hirai et al., 1979; Okano et al., 1985; Mousli et al., 1989; Katsu et al., 1990), enhance phospholipase A_2 activity (Argiolas & Pisano, 1986), kill *Staphylococcus aureus* (Katsu et al., 1990), and facilitate the opening of the mitochondrial permeability transition pore (Pfeiffer et al., 1995). These activities are considered to be closely related to their interactions with membranes. The peptides bind to phospholipid membranes, forming amphiphilic helices (Higashijima et al., 1983; Wakamatsu et al., 1983, 1992; Schwarz & Blochmann, 1993), which perturb the lipid bilayers, leading to membrane permeabilization (Katsu et al., 1990; Tanimura et al., 1991; Danilenko et al., 1993; Pfeiffer et al., 1995; Schwarz & Arbuzova, 1995). At high ionic strength (≥0.3 M), mastoparans are known to form ion channels in planar lipid bilayers (Mellor & Sansom, 1990). As for histamine release, it has been shown that they directly interact with and activate pertussis toxin-sensitive G-proteins *in vitro* in a manner very similar to that of G-protein-coupled receptors (Higashijima et al., 1988, 1990; Mousli et al., 1990). Therefore, the peptides should rapidly pass through the cell membranes to react with the cytoplasmic proteins. However, the permeation of mastoparans per se across the lipid bilayers has never been tested.

We have recently reported that magainin 2, an antimicrobial peptide found in *Xenopus laevis*, translocates into lipid vesicles by forming a short-lived pentameric pore as an intermediate (Matsuzaki et al., 1995a,b). Magainin 2 is similar to mastoparans in that the former peptide forms an amphiphilic helix, permeabilizing the lipid bilayers (Matsuzaki et al., 1991, 1994). Ion channel formation is again observed (Cruciani et al., 1992). Thus; it is highly probable that mastoparans also translocate across the bilayers accompanying pore formation. It is quite important in understanding peptide−lipid interactions to clarify whether this mechanism is specific to magainin 2 or more universal.

In the first part of this paper, we studied the pore formation of mastoparan X from *Vespa xanthoptera* (Okumura et al., 1981) Ile-Asn-Trp-Lys-Gly-Ile-Ala-Ala-Met-Ala-Lys-Lys-Leu-Leu-NH_2. We measured the efflux of a self-quenching dye, calcein, entrapped within large unilamellar vesicles (LUVs)[1] (Matsuzaki et al., 1994). This method also provides information on the lifetime of the pore. In the second part, we investigated the transbilayer movement of the peptide by three different experiments. The first two experiments quantitated the amount of the untranslocated peptide remaining in the outer monolayers of LUVs by use of fluorescence resonance energy transfer (RET) from the Trp^3 residue to a dansylated lipid in the membrane phase (Matsuzaki et al., 1995a). The third procedure more directly proved the translocation. The pore formation by mastoparan X in the inner bilayers of multilamellar vesicles (MLVs) was monitored based on the reduction of an NBD lipid by sodium dithionite (Matsuzaki et al., 1995b). Furthermore, the coupling between the translocation and the pore formation was examined. Finally, we found that mastoparan X induces a pore-mediated rapid flip-flop of the membrane lipids, as found for magainin 2 (Matsuzaki, K., et al., manuscript submitted). We discuss a plausible mechanism for the

† Supported by Grant-in-Aids (No. 08219223 and No. 08772061) from the Ministry of Education, Science and Culture of Japan.

* Author to whom correspondence should be addressed. Telephone: 81-75-753-4574. Fax: 81-75-761-2698. E-mail: katsumim@pharmsun.pharm.kyoto-u.ac.jp.

⊗ Abstract published in *Advance ACS Abstracts,* June 1, 1996.

[1] Abbreviations: LUVs, large unilamellar vesicles; MLVs, multilamellar vesicles; RET, resonance energy transfer; egg PC, egg yolk L-α-phosphatidylcholine; egg PG, L-α-phosphatidyl-DL-glycerol enzymatically converted from egg PC; DNS-PE, *N*-[[(5-(dimethylamino)-naphthyl]-1-sulfonyl]dipalmitoyl-L-α-phosphatidylethanolamine; C_6-NBD-PC, 1-palmitoyl-2-[6-((7-nitrobenz-2-oxa-1,3-diazol-4-yl)amino)-caproyl]-L-α-phosphatidylcholine; NBD-PE, *N*-[(7-nitrobenz-2-oxa-1,3-diazol-4-yl)dipalmitoyl]-L-α-phosphatidylethanolamine; P/L, peptide-to-lipid molar ratio.

S0006-2960(96)00342-X CCC: $12.00

coupled transbilayer transport of the peptides, ions, and lipids.

MATERIALS AND METHODS

Materials. Synthetic mastoparan X was purchased from Bachem (Bubendorf, Switzerland). The concentration of the stock solution was routinely determined based on Trp absorbance at 280 nm. Egg yolk L-α-phosphatidylcholine (egg PC) was purchased from Sigma. L-α-Phosphatidyl-DL-glycerol (egg PG) enzymatically converted from egg PC was a kind gift from Nippon Fine Chemical Co. (Takasago, Japan). 1-Palmitoyl-2-[6-((7-nitrobenz-2-oxa-1,3-diazol-4-yl)amino)caproyl]-L-α-phosphatidylcholine (C_6-NBD-PC) was obtained from Avanti Polar Lipids (Alabaster, AL). *N*-[[5-(Dimethylamino)naphthyl]-1-sulfonyl]dipalmitoyl-L-α-phosphatidylethanolamine (DNS-PE) and *N*-[(7-nitrobenz-2-oxa-1,3-diazol-4-yl)dipalmitoyl]-L-α-phosphatidylethanolamine (NBD-PE) were products of Molecular Probes (Eugene, OR). Calcein and spectrograde organic solvents were supplied by Dojindo (Kumamoto, Japan). All other chemicals from Wako (Tokyo, Japan) were of special grade. A Tris-HCl buffer (10 mM Tris/150 mM NaCl/1 mM EDTA, pH 7.0) was prepared from water twice distilled in a glass still.

Vesicle Preparation. LUVs were prepared by extrusion of MLVs, as described elsewhere (Matsuzaki et al., 1994). Briefly, a lipid film, after being dried under vacuum overnight, was hydrated with a 70 mM calcein solution for the dye release assay (pH was adjusted to 7.0 with NaOH) or the Tris buffer for the other experiments and vortex mixed to produce MLVs. The suspension was freeze−thawed for five cycles and then successively extruded through polycarbonate filters (a 0.6 μm pore size filter, five times; two stacked 0.1 μm pore size filters, 10 times). The lipid concentration was determined in triplicate by phosphorus analysis (Bartlett, 1959).

Leakage. The calcein-entrapped LUVs were separated from free calcein on a Bio-Gel A-1.5m column. The release of calcein from LUVs was fluorometrically monitored at an excitation wavelength of 490 nm and an emission wavelength of 520 nm on a Shimadzu RF-5000 spectrofluorometer whose cuvette holder was thermostated at 30 ± 0.5 °C. The maximum fluorescence intensity corresponding to 100% leakage was determined by the addition of 10% Triton X-100 (20 μL) to 2 mL of the sample. The reported time courses of the leakage were the average of three experiments, and the standard deviations were indicated by error bars. The mode of leakage was examined, as described earlier (Matsuzaki et al., 1994; see also the text).

Peptide Binding. The binding affinity of the peptide for the membrane was determined on the basis of Trp fluorescence. Mastoparan X solutions (3 μM) containing various amounts of LUVs were incubated at 30 °C overnight to reach binding equilibrium. Fluorescence spectra in the range of 300−400 nm were measured at an excitation wavelength of 280 nm on a Hitachi F-4500 spectrofluorometer. The spectra were corrected for both wavelength-dependent effects (Melhuish, 1962) and intensity loss due to light scattering after subtraction of the corresponding blank spectra without the peptide. The latter correction was carried out by use of indoxyl sulfate (Matsuzaki et al., 1994).

Resonance Energy Transfer (RET). Symmetrically labeled LUVs were prepared by hydrating the lipid film composed of egg PC, egg PG, and DNS-PE in a molar ratio of 7:2:1. RET from the Trp residue of the peptide to the dansyl chromophore in the membrane was monitored by observing the fluorescence intensity of either the Trp residue (336 nm) or the dansyl group (510 nm) upon excitation at 280 nm. The temperature was controlled at 30 ± 0.5 °C.

Inner Leaflet-Labeled Vesicles. NBD-labeled LUVs were generated from a 7:3 mixture of egg PC and egg PG containing 1 mol % NBD-PE or C_6-NBD-PC as described above. The symmetrically labeled vesicles were mixed with sodium dithionite ([lipid] = 8 mM, [dithionite] = 60 mM) and incubated for 15 min at 30 °C. Only the NBD groups in the outer leaflets of the bilayers were chemically quenched by dithionite reduction (McIntyre & Sleight, 1991; see also Figure 7). The vesicles were immediately separated from dithionite by gel-filtration (Bio-Gel A-1.5 m, 1.5 × 18 cm column) at 4 °C.

Outer Leaflet-Labeled Vesicles. LUVs composed of egg PC/egg PG (7:3) were prepared as described above (4.25 mM × 3 mL). C_6-NBD-PC dissolved in ethanol (60 μL of an 1.06 mM solution, corresponding to 1% of the outer monolayer lipids of the LUVs) was added to the LUVs with stirring. The vesicles were incubated for 1 h for equilibration. The asymmetric labeling was almost perfect, because addition of sodium dithionite quenched 95% of the NBD fluorescence.

Detection of Flip-Flop. The fraction of the NBD-lipids which had flipped or flopped during the incubation in the absence or presence of mastoparan X was measured on the basis of fluorescence quenching by sodium dithionite. The asymmetrically NBD-labeled LUVs were incubated with or without the peptide at 30 °C for various times. In the case of the peptide-containing samples, 20 μL of a trypsin solution (5 mg/mL) was added and reacted for 4 min in order to hydrolyze the peptide. After 20 μL of 1 M sodium dithionite had been added to 2.02 mL of a sample, NBD fluorescence was monitored at 30 ± 0.5 °C. The excitation and emission wavelengths were 450 and 530 nm, respectively. Fluorescence intensity, F, was normalized to the intensity prior to dithionite addition, F_0.

RESULTS

Pore Formation (Ion Movement). The ion movement, i.e., the formation of some kind of pore, was detected based on the efflux of an anionic fluorescent dye, calcein, from liposomes (Matsuzaki et al., 1994). The dye release was observed as an increase in fluorescence intensity because of relief from the self-quenching of the dye molecules concentrated (70 mM) within the LUVs. To convert the fluorescence signal to the extent of leakage value, the mode of leakage or the lifetime of the pore should be determined (Weinstein et al., 1984). If the lifetime is much longer than ca. 10 ms (Matsuzaki et al., 1995b), a single pore opening is sufficient to exhaust the vesicular contents ("all-or-none mode"). On the other hand, a number of pore openings are necessary to observe a significant extent of leakage in the case of a pore with a much shorter lifetime ("graded mode"). In the latter mode, fluorescence from intravesicular diluted calcein should make a nontrivial contribution to the measured fluorescence. These two modes can be distinguished by determination of the percent self-quenching value of the intravesicular dye after the peptide treatment. After incuba-

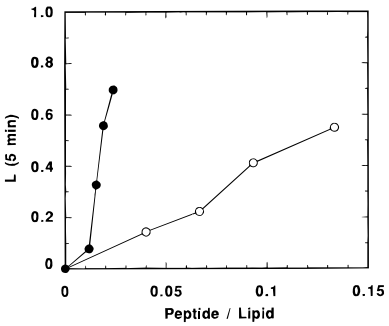

FIGURE 1: Pore formation induced by mastoparan X. Pore formation was estimated by the leakage of an anionic, fluorescent dye, calcein, from LUVs composed of egg PC/egg PG. The percent leakage value after 5-min incubation was plotted against the peptide-to-lipid molar ratio. Each value is the average of duplicated experiments. Egg PG contents: ○, 5 mol %; ●, 30 mol %. The temperature of all experiments was controlled at 30 ± 0.5 °C.

tion of egg PC/egg PG (7:3) LUVs with the peptide for 10 min ([peptide] = 2.5 μM, [lipid] = 151 μM), the vesicle fraction was separated from leaked calcein by gel filtration, and its percent self-quenching value was obtained by measuring the fluorescence intensity before and after addition of Triton X-100. The observed value, 63.3 ± 4.2% was much closer to the predicted value of 68.9 ± 4.0% in the case of the graded-mode rather than the value (89.2%) for the all-or-none mode, suggesting a short-lived pore. The details of the calculation have been described elsewhere (Matsuzaki et al., 1994).

Figure 1 shows the extent of leaked calcein during 5-min incubation as a function of P/L. An increase in PG content from 5% to 30% resulted in a drastic enhancement of pore formation. Furthermore, the dose−response curve at 30% PG appeared to have a threshold value around a P/L of 0.01, indicative of the cooperative nature of the pore formation process (see also Figure 8).

Binding Affinity. In order to clarify the role of PG in the pore formation, we examined the effect of the anionic lipid on the membrane binding affinity of the peptide. Figure 2 depicts the spectral change in the Trp residue upon lipid addition. The binding caused a blue-shift from 348 to 327−333 nm (Figure 2A) concomitant with intensity increase (Figure 2B), suggesting that the Trp residue is buried in a more hydrophobic environment upon membrane binding. These spectral changes were more pronounced in the PG containing membranes than in the pure PC vesicles. The presence of 30% PG (closed circles) significantly enhanced the binding affinity, because the maximal spectral change was attained at a lower lipid concentration.

Peptide Translocation. In the first two experiments, the translocation was detected by measuring the amount of the untranslocated peptides remaining in the outer monolayers (Matsuzaki et al., 1995a). The untranslocated peptides can be readily removed from the vesicle surface either by degradation with a protease, trypsin, or by extraction with a large excess of a second population of vesicles.[2] The unremovable fraction was determined by use of RET from the Trp residue of mastoparan X to the dansyl chromophore (DNS-PE) incorporated into the membrane phase.

Figure 3 depicts the results by the first procedure. Trypsin hydrolyzes the peptide bonds on the C-terminal sides of the Lys residues. The hydrolyzed Trp-containing fragment, Ile-Asn-Trp[3]-Lys, will be desorbed from the membrane and can be detected by the RET technique; the desorption results in relief from RET, i.e., a decrease in dansyl fluorescence at 510 nm when excited at 280 nm, where Trp is selectively excited. The enzyme was added to a peptide solution that had been incubated with dansyl-labeled vesicles for various times. Simultaneous addition of the protease and the vesicles to the peptide solution digested the peptide molecules and almost completely desorbed the Trp-containing fragment from the membrane within 3 min (trace 1), whereas prolonged preincubation partially protected the peptide from the enzyme attack (traces 2−4). These results show that the peptide becomes less exposed in a time-dependent manner, suggesting the possibility that the peptide molecules translocate into the inner leaflet across the bilayer. They also indicate that the mastoparan X-induced pore is not large enough for the enzyme (MW 24 000) to pass through. The $\Delta F/F_0$ value is a direct measure of the fraction of the translocated peptide.

Figure 4 exhibits the data by the second protocol. The addition of dansyl-labeled vesicles to a peptide solution at time zero resulted in a significant decrease in Trp fluorescence from F_1 to F_2, indicating RET due to the binding of the peptide to the membrane. After a short incubation for 0.5 min, a second population of dansyl-free vesicles (DNS-PE was substituted by egg PG) was added in large excess (trace 2). An increase in the fluorescence intensity implies that the peptide molecules, which had been bound to the *outer* leaflet, were redistributed between the two vesicle populations, resulting in relief from RET. The increased fluorescence intensity, however, was smaller than F_0', the intensity when both populations of vesicles were added simultaneously to the peptide solution at time zero (trace 1), suggesting that a fraction of the peptides, which is related to $\Delta F'$, became unexposed to the outer surface and therefore untransferable to the second vesicles. The buried fraction increased with the incubation time (traces 2−6), reinforcing the conclusion from Figure 3. These fluorescence intensities were determined 3 min after the addition of the second vesicles for comparison with the data from Figure 3.

Figure 5 more directly proves the peptide translocation. Addition of sodium dithionite to MLVs doped with NBD-PE reduced the chromophores exposed to the external aqueous phase, making them nonfluorescent (trace 1). The fluorescence decrease was biphasic, as reported elsewhere (McIntyre & Sleight, 1991). The slower phase corresponds to the slow permeation of the reducing ions through the bilayers. The linear extrapolation to time zero (broken line) estimated the fraction of the NBD groups on the vesicular surface to be 25%, indicating that the lamellarity of the vesicle is 2 or larger: the anionic bilayers tend to be swelled because of electrostatic repulsion and the circumference of each lamellar grows significantly as one goes out from the center. The external addition of mastoparan X (trace 2) allowed the reducing ion to react with more than 90% NBD groups within 6 min; the peptide molecules translocated across the outermost bilayers to form pores in the *inner bilayers*. If the peptide had permeabilized only the outer

[2] In these studies, we used liposomes containing 30 mol % acidic phospholipids, which are necessary for the effective binding of the peptide. However, the incorporation of more than 50 mol % acidic lipids inhibited the rapid removal of the untranslocated peptides with the enzyme or the vesicles because of the excessively strong binding.

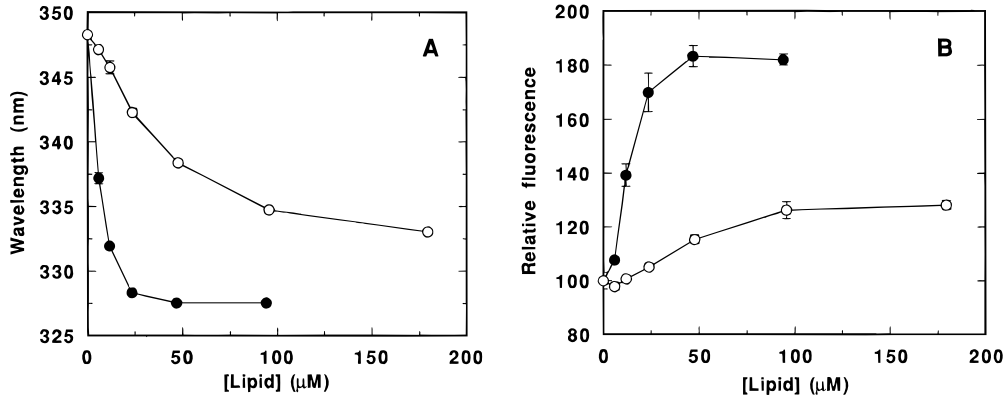

FIGURE 2: Binding affinity of mastoparan X. The peptide (3 μM) was incubated with LUVs at 30 °C overnight for equilibration. Fluorescence spectra were measured at an excitation wavelength of 280 nm. The maximal wavelength (A) and intensity (B) are plotted againt the lipid concentration. The plotted values are the average of duplicated samples. Lipid composition: ○, egg PC; ●, egg PC/egg PG (7:3).

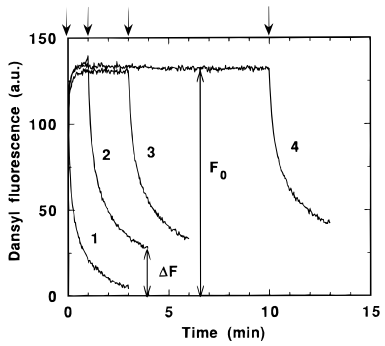

FIGURE 3: Detection of the peptide translocation (1). Trypsin (final concentration, 25 μg/mL) was added to a mastoparan X solution which had been incubated with dansyl-labeled vesicles (egg PC/egg PG/DNS-PE, 7:2:1, molar ratio) for various times, as indicated by the arrows. The peptide and lipid concentrations were 3 and 113 μM, respectively. The fluorescence intensity of the dansyl chromophore at 510 nm (excited at 280 nm) was recorded. The binding of the peptide increases fluorescence due to RET. Simultaneous addition of trypsin and the vesicles to the peptide solution digested the peptide molecules and completely desorbed them from the membrane within 3 min (trace 1), whereas prolonged preincubation (for 1, 3, or 10 min) protected the peptide from enzyme attack (traces 2−4). $\Delta F/F_0$ corresponds to the fraction of the translocated peptide. Each trace is the average of three experiments.

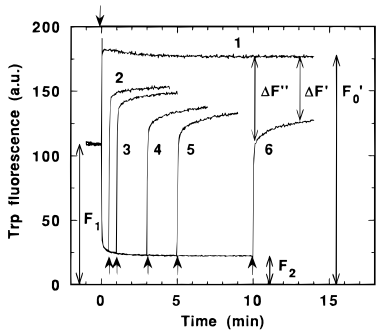

FIGURE 4: Detection of the peptide translocation (2). Mastoparan X was mixed with dansyl-LUVs (egg PC/egg PG/DNS-PE = 7:2:1) at time zero. The final peptide and lipid concentrations were the same as in Figure 3. The fluorescence intensity of Trp at 336 nm (excited at 280 nm) was recorded. The binding of the peptide to the vesicle reduced the intensity from F_1 to F_2 due to RET. At various time intervals of incubation (0.5, 1, 3, 5, 10 min, traces 2−6), a large excess (final concentration 686 μM) of the second population of dansyl-free LUVs (egg PC/egg PG = 7:3) was added, as indicated by the arrows. An increase in intensity indicates the relief from RET caused by the redistribution between the two vesicle populations of the peptide molecules which had been bound to the outer surface of the first vesicle. The increased intensity decreases with prolonged incubation and is smaller than the fluorescence intensity (F_0') when both populations of vesicles were simultaneously added at time zero (trace 1), thus indicating that some of the peptides translocated into the inner leaflet during the incubation. Each trace is the average of three experiments.

most bilayers, the reagent could have reacted with the chromophores facing the first interlamellar space, having resulted in quenching less than 75%.

Coupling between Pore Formation and Translocation. The extent of leakage value, L, was determined under the conditions identical to those of Figures 3 and 4. Figure 6 summarizes the relationship between the pore formation and the peptide translocation. The latter was expressed as the mole of the translocated peptide per mole of the total lipid, r_i, which was calculated either by ΔF[P]/F[L] from Figure 3 (closed circles) or $\Delta F'$[P]/($F_0' - F_2$)[L] (Matsuzaki et al., 1995a) from Figure 4 (open circles).[3] The concentrations of the peptide and the lipid were denoted by [P] and [L], respectively. The agreement between the r_i values estimated from the two different experiments was remarkable. The L value was proportional to r_i. In other words, the pore formation was coupled with the peptide internalization.

$$L = \alpha r_i \quad (1)$$

The α values were estimated to be 68.4 ± 2.4 (R = 0.923) from Figure 3 and 72.2 ± 0.8 (R = 0.986) from Figure 4. These values seem to be overestimated because some peptides could back-translocate from the inner to the outer monolayer within 3 min. If the r_i value was estimated based on the initial abrupt increase in fluorescence intensity upon addition of the second population of vesicles ($\Delta F''$ in Figure 4), the α value was 57.1 ± 0.8 (R = 0.976, open squares).

Lipid Flip-Flop. The peptide induced enhancement of lipid flip-flop was again determined by use of the NBD−dithionite reaction. This method is based on the fact that the intact lipid bilayer is essentially impermeable to the

[3] This calculation implicitly assumes complete binding of the peptide. The minimum unbound fraction, or the maximum error in the estimation in r_i, would be F_2/F_1 = ca. 0.2, even if the peptide bound to the dansyl-labeled vesicles emitted no fluorescence. However, the fractional quenching in the dansyl-labeled LUVs is estimated to be 0.86 under our experimental conditions (a dansyl chromophore per 680 Å^2 and a critical transfer distance of ca. 20 Å for the Trp-dansyl pair) according to Wolber and Hudson (1979). Therefore, the fluorescence, F_2, mainly originates from the peptide bound to the dansyl-labeled vesicles ($F_2 \approx F_0' \times 0.14$), indicating complete membrane binding. See also Figure 2.

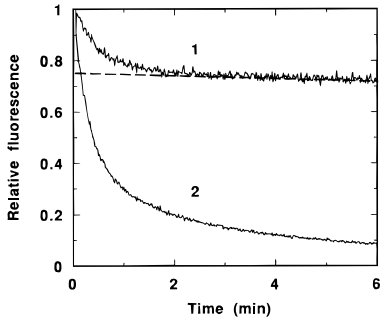

FIGURE 5: Detection of the peptide translocation (3). Small aliquots of MLVs composed of egg PC/egg PG/NBD-PE (7:3:0.05) were injected into a buffer (curve 1) or a mastoparan X solution (curve 2) in the presence of 10 mM sodium dithionite. The essentially membrane-impermeable ion chemically quenches the NBD fluorescence. The fluorescence at 530 nm (excitation at 450 nm) was normalized to the intensity in the absence of the reducing ion. The peptide makes almost all NBD groups accessible to the $S_2O_4^{2-}$ ion, suggesting that it passes through the outermost bilayers to form pores in the inner bilayers. [lipid] = 58.9 μM, [peptide] = 3 μM.

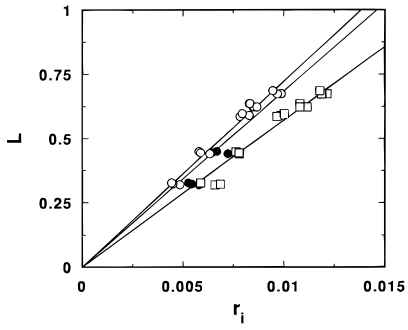

FIGURE 6: Relationship between pore formation and peptide translocation. The pore formation was estimated on the basis of the leakage of calcein from 30 mol % egg PG containing LUVs (Figure 1). The extent of leakage is denoted by *L*. The translocation was evaluated by the two methods in Figures 3 and 4 and expressed as r_i, the moles of the translocated peptide in the inner leaflet per mole of the lipid in the bilayer. Results from 2−3 experiments are plotted. The r_i value was calculated from ●, $\Delta F/F_0$ in Figure 3; ○, $\Delta F'$ in Figure 4; □, $\Delta F''$ in Figure 4. The lines are the regression lines.

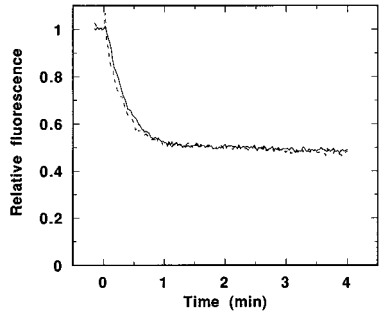

FIGURE 7: Stopping of mastoparan X-induced membrane permeabilization by trypsin. Small aliquots of egg PC/egg PG (7:3) LUVs doped with 0.5 mol % NBD-PE were added to a 10 mM sodium dithionite buffer solution. The NBD fluorescence was monitored, as in Figure 5 (solid line). The dotted line shows the quenching kinetics when the sample was treated with trypsin (50 μg/mL) for 4 min after the vesicles (120 μM) had been incubated with 3 μM mastoparan X for 5 min.

reducing ion. However, mastoparan X forms pores in the membrane, as shown in Figures 1 and 5. To overcome this difficulty, trypsin was used to deactivate the peptide. The broken line in Figure 7 depicts the time course of the NBD reduction of symmetrically labeled LUVs after the enzyme

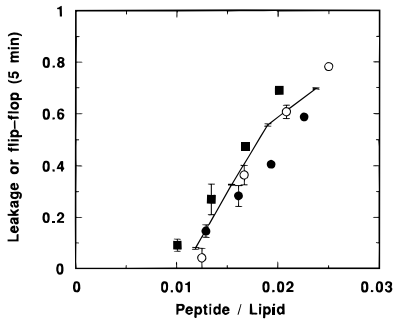

FIGURE 8: Dose−response curves of mastoparan X-induced ion permeation and lipid flip-flop. Leakage of calcein and flip-flop of NBD-labeled lipids during 5 min were investigated for egg PC/egg PG (7:3) LUVs. Extent of calcein leakage is plotted as a solid line. Symbols represent percent flip-flop of NBD-lipids, as determined by use of the NBD-dithionite reaction. ■, inner leaflet-labeled NBD-PE; ●, inner leaflet-labeled NBD-PC; ○, outer leaflet-labeled NBD-PC. Plotted data are the average of duplicated experiments.

treatment in the presence of the peptide. The kinetics was superimposable on that of the peptide-free sample (solid line), guaranteeing that the enzyme does stop the membrane permeabilization. Furthermore, Figure 7 shows that the vesicles we used are unilamellar (50% quenching).

Figure 8 shows the dose−response curves of calcein leakage and lipid flip flop triggered by mastoparan X. The extent of flip-flop was calculated according to

$$\text{flip-flop} = (n_0 - n)/(n_0 - n_\infty) \qquad (2)$$

where n_0, n, and n_∞ represent the fractions of inner-located lipids in asymmetric LUVs without the peptide, asymmetric LUVs with the peptide, and symmetric LUVs without the peptide, respectively. The peptide induced the transbilayer movement of both the negatively charged (*N*-NBD-PE, squares) and zwitterionic (C_6-NBD-PC, circles) lipid probes above P/L of 0.01. The flip-flop of the former was slightly faster. The initial labeling condition (inner-leaflet labeling or outer-leaflet labeling) did not affect the results (open versus closed circles). Interestingly, the leakage (solid line) was observed in the same peptide concentration range, i.e., the pore formation was coupled with the lipid flip-flop.

DISCUSSION

Membrane Binding. Mastoparans exhibit affinity for lipid bilayers and form amphiphilic helices in membranous environments (Higashijima et al., 1983; Wakamatsu et al., 1983, 1992; Katsu et al., 1990; De Kroon et al., 1991; Schwarz & Blochmann, 1993; Fujita et al., 1994; Schwarz & Arbuzova, 1995). The presence of acidic phospholipids strengthens the interactions (De Kroon et al., 1991), in agreement with our results (Figures 1 and 2). One of the roles of PG is the electrostatic enhancement of peptide binding (Figure 2). Desensitization of mast cells by neuraminidase treatment (Mousli et al., 1989), i.e., sialic acid removal, may be understandable on the basis of the reduction in electrostatic attractions. Furthermore, the presence of PG appears to allow a deeper penetration of the peptide, as judged from the larger extent of blue-shift and quantum yield enhancement. Similar phenomena were found for a bee venom, melittin (Batenburg et al., 1987). However, another acidic lipid, cardiolipin, is reported to prevent the deep insertion of mastoparan X (De Kroon et al., 1991). The

mode of the peptide−lipid interactions may depend not only on the lipid charge but also on its chemical nature.

The mastoparan helix in the PC bilayers is suggested to lie parallel to the membrane surface and form an aggregate (Fujita et al., 1994). The Trp fluorescence data (Figure 2) are compatible with this scheme. The maximal wavelength of the membrane-bound peptide (327 nm) indicates that the environment of the fluorophore is not completely hydrophobic (Cowgill, 1967). A minimum in fluorescence intensity was observed at the smallest PC concentration (Figure 2B). One explanation would be that the fluorescence of the membrane-bound peptide is quenched because of strong interpeptide interactions.

Pore Formation. After membrane binding, the peptides are known to enhance the permeability of both artificial (Katsu et al., 1990; Mellor & Sansom, 1990; Pfeiffer et al., 1995; Schwarz & Arbuzova, 1995) and biological membranes (Katsu et al., 1990; Tanimura et al., 1991; Danilenko et al., 1993; Pfeiffer et al., 1995). Mastoparan X appears to form a pore of definite size. Dithionite (MW 128, Figure 5) and calcein (MW 623, Figure 1) are permeable but trypsin (MW 24 000) is not (Figure 3). The size of the pore depends on the P/L value. Our preliminary study showed that a fluorescent dextran of MW 4400 is impermeable below P/L = 0.05 where calcein is highly permeable (Figure 1), whereas the polymer becomes permeable at higher P/L ratios of 0.05−0.1 (Matsuzaki, K., et al., unpublished work). Therefore, the radius of the pore is estimated to be 5−10 Å below P/L = 0.05.

The leakage of calcein supralinearly depends on the peptide concentration in the membrane containing 30% PG (Figure 1), suggesting that the pore is composed of several peptide molecules. Our kinetic experiments on calcein leakage using a stopped-flow apparatus showed that the initial leakage rate was approximately proportional to the fifth power of the peptide concentration (Matsuzaki, K., et al., unpublished work). This molecularity agrees with the value estimated for the ion channel formed by mastoparan, a related peptide (Mellor & Sansom, 1990). However, the time course of leakage was sigmoidal in the very initial phase, indicating that the binding of the peptide to the membrane is not sufficiently fast, in keeping with a relatively slow initial increase in dansyl fluorescence (Figure 3).

The pore structure has been modeled as a bundle of membrane-spanning helices with their hydrophilic surfaces oriented toward the central aqueous pore (Mellor & Sansom, 1990). A helix composed of 14 amino acid residues is 21 Å long, being shorter than the hydrophobic thickness of the bilayer (ca. 30 Å). A nuclear magnetic resonance study (Wakamatsu et al., 1992) revealed that the two N-terminal residues of membrane-bound mastoparan X do not form a helix, making the length of the whole peptide longer. This conclusion was supported by circular dichroism measurements (Schwarz & Blochmann, 1993). The ellipticity at 222 nm of membrane-associated mastoparan X in the presence of 0.1−0.4 M NaCl is −19 000 deg cm^2 dmol^{-1}, indicating that the helicity is lower than 100%. In contrast, the ellipticity of mastoparan is −30 000 in the absence of the salt. The ion channel formation by the latter peptide (Mellor & Sansom, 1990) requires the addition of salt (≥0.3 M), which reduces the negative ellipticity to ca. −20 000 (Schwarz & Blochmann, 1993). Therefore, the pore appears to be composed of a bundle of partially unraveled helices. Furthermore, the bilayer in the liquid-crystalline phase can be locally deformed to match its hydrophobic thickness to the peptide length. It is also plausible that surface-lying amphiphilic helices, i.e., preaggregates, perturb the bilayer to thin the membrane (Ludtke et al., 1995). Another possibility is that a bundle of dimeric peptides (e.g., head-to-tail dimer) constitutes a pore. The helix bundle model is not incompatible with the parallel orientation of the helix because of the transient nature of the pore formation, as discussed for magainin 2 (Matsuzaki et al., 1995a).

The lifetime of the pore, τ, was estimated to be much shorter than τ_0, the pore opening time necessary for a 1/e reduction in the concentration of the intravesicular contents, because the calcein leakage occurred in the graded mode. This conclusion is in keeping with the observation of $\alpha \approx 60$ in eq 1 (Matsuzaki et al., 1995b). Schwarz and Arbuzova (1995) found that the τ value of a mastoparan X pore in palmitoyloleoylphosphatidylcholine LUVs is comparable to τ_0. The τ_0 value is proportional to the solute size and inversely proportional to pore area (Schwarz & Robert, 1990). They used carboxyfluorescein as a fluorescent marker. It is reported that this anionic dye itself readily permeates the lipid bilayer, and the impermeability of its counter ion (Na^+) retains the dye within the vesicle (Bramhall, 1984). Therefore, a sodium-permeable, small pore is sufficient to allow the dye to leak. The pore they discussed may be different in size (accordingly, τ_0) from ours. It is also plausible that the incorporation of PG modulates the pore stability, because the pore structure appears to involve lipids (vide infra).

Translocation. The peptide translocation was coupled with the pore formation (Figure 6). This fact can be explained as follows (Matsuzaki et al., 1995a). The peptide molecules first reside on the outer monolayer. They form membrane-spanning pores of short duration. Upon their disintegration, a fraction of the peptides stochastically translocate into the inner leaflet. A reduction in the peptide density in the outer monolayer slows the pore formation rate because of the cooperative nature of the pore formation. Figures 3 and 4 show that the translocation rate is initially fast but subsequently reduced. The initial quick internalization of the peptide due to the short lifetime can explain the rapid kinetics of histamine release (Okano et al., 1985). Analog peptides having shorter pore lifetimes would effectively enter the cells without significantly permeabilizing the cell membranes (Danilenko et al., 1993).

The translocation of the positively charged peptide will be facilitated by an inside negative transmembrane potential, as found for magainin 2 (Matsuzaki et al., 1995c). The potential was reported to increase the membrane permeabilization (Pfeiffer et al., 1995). Moreover, the observation that the application of the potential enhances the membrane binding of mastoparan X in a time-dependent manner (De Kroon et al., 1991) may be interpreted as a consequence of the peptide translocation.

Flip-Flop. Mastoparan X induced the flip-flop of both NBD-PE and NBD-PC on a time scale of minutes (Figure 8). Its rate was independent of the initial labeling conditions. These results indicate that the peptide rapidly randomizes all the lipids in the membranes. We reject a model in which a solid peptide−lipid complex moves from the outer to inner leaflets, because the peptide almost unidirectionally translocates from the outer to the inner leaflet, whereas the lipid

is transferred in both directions at the same velocity. The stoichiometry also argues against the model. Figure 8 shows that at P/L = 0.02, for example, the extent of flip-flop is ca. 0.6, corresponding to 55 000 lipid molecules being scrambled (90 000 lipid molecules constitute a 100-nm LUV). Because L is also 0.6, the r_i value is 0.01 (eq 1); that is, 900 peptide molecules translocate into the inner leaflet. A single peptide would have to accompany 60 lipid molecules.

The coupling between the flip-flop and pore formation (Figure 8) suggests a "pore-mediated flip-flop" (Fattal et al., 1994). We found similar phenomena for an antimicrobial peptide, magainin 2, and postulated a novel model in which the lipids are also involved in the pore structure with their head groups constituting the pore lining (Matsuzaki, K., et al., manuscript submitted). Such a situation makes the outer and inner monolayers a continuum, allowing the lipid molecules to freely diffuse. A theoretical treatment has also been discussed.

In summary, mastoparan X mediates the simultaneous transbilayer transport of ions and lipids coupled with the translocation of the peptide itself. This mechanism appears to be universal: similar phenomena were also observed for magainin 2 (Matsuzaki et al., 1995a,b). Melittin and GALA peptides also induce the flip-flop in a pore-mediated manner (Fattal et al., 1994), although it is still unclear if they translocate across the lipid bilayers in the absence of a transmembrane potential. A mitochondrial presequence peptide is reported to pass through and permeabilize the membrane (Roise et al., 1986; Maduke & Roise, 1993). It could cause the lipid randomization. Thus, peptide−lipid interactions are rather more dynamic than had been thought. Furthermore, there is a quantitative relationship or coupling between the transbilayer traffic of the peptides, ions, and lipids.

REFERENCES

Argiolas, A., & Pisano, J. J. (1986) *J. Biol. Chem. 258*, 13697−13702.

Bartlett, G. R. (1959) *J. Biol. Chem. 234*, 466−468.

Batenburg, A. M., Hibbeln, J. C. L., & de Kruijff, B. (1987) *Biochim. Biophys. Acta 903*, 155−165.

Bramhall, J. (1984) *Biochim. Biophys. Acta 778*, 393−399.

Cowgill, R. W. (1967) *Biochim. Biophys. Acta 133*, 6−18.

Cruciani, R. C., Barker, J. L., Durell, S. R., Raghunathan, G., Guy, H. R., Zasloff, M., & Stanley, E. F. (1992) *Eur. J. Pharmacol.-Mol. Pharmacol. Sect. 226*, 287−296.

Danilenko, M., Worland, P., Carlson, B., Sausville, E. A., & Sharoni, Y. (1993) *Biochem. Biophys. Res. Commun. 196*, 1296−1302.

De Kroon, A. I. P. M., de Gier, J., & de Kruijff, B. (1991) *Biochim. Biophys. Acta 1068*, 111−124.

Fattal, E., Nir, S., Parente, R. A., & Szoka, F. C., Jr. (1994) *Biochemistry 33*, 6721−6731.

Fujita, K., Kimura, S., & Imanishi, Y. (1994) *Biochim. Biophys. Acta 1195*, 157−163.

Higashijima, T., Wakamatsu, K., Takemitsu, M., Fujino, M., Nakajima, T., & Miyazawa, T. (1983) *FEBS Lett. 152*, 227−230.

Higashijima, T., Uzu, S., Nakajima, T., & Ross, E. M. (1988) *J. Biol. Chem. 263*, 6491−6494.

Higashijima, T., Burnier, J., & Ross, E. M. (1990) *J. Biol. Chem. 265*, 14176−14186.

Hirai, Y., Yasuhara, T., Yoshida, H., Nakajima, T., Fujino, M., & Kitada, C. (1979) *Chem. Pharm. Bull. 27*, 1942−1944.

Katsu, T., Kuroko, M., Morikawa, T., Sanchika, K., Yamanaka, H., Shinoda, S., & Fujita, Y. (1990) *Biochim. Biophys. Acta 1027*, 185−190.

Ludtke, S., He, K., & Huang, H. (1995) *Biochemistry 34*, 16764−16769.

Maduke, M., & Roise, D. (1993) *Science 260*, 364−367.

Matsuzaki, K., Harada, M., Funakoshi, S., Fujii, N., & Miyajima, K. (1991) *Biochim. Biophys. Acta 1063*, 162−170.

Matsuzaki, K., Murase, O., Tokuda, H., Funakoshi, S., Fujii, N., & Miyajima, K. (1994) *Biochemistry 33*, 3342−3349.

Matsuzaki, K., Murase, O., Fujii, N., & Miyajima, K. (1995a) *Biochemistry 34*, 6521−6526.

Matsuzaki, K., Murase, O., & Miyajima, K. (1995b) *Biochemistry 34*, 12553−12559.

Matsuzaki, K., Sugishita, K., Fujii, N., & Miyajima, K. (1995c) *Biochemistry 34*, 3423−3429.

McIntyre, J. C., & Sleight, R. G. (1991) *Biochemistry 30*, 11819−11827.

Melhuish, W. H. (1962) *J. Opt. Soc. Am. 52*, 1256−1258.

Mellor, I. R., & Sansom, M. S. P. (1990) *Proc. R. Soc. London B 239*, 383−400.

Mousli, M., Bronner, C., Bueb, J.-L., Tschirhart, E., Gies, J.-P., & Landry, Y. (1989) *J. Pharmacol. Exp. Ther. 250*, 329−335.

Mousli, M., Bueb, J.-L., Bronner, C., Rouot, B., & Landry, Y. (1990) *Trends Pharmacol. Sci. 11*, 358−362.

Okano, Y., Takagi, H., Tohmatsu, T., Nakashima, S., Kuroda, Y., Saito, K., & Nozawa, Y. (1985) *FEBS Lett. 188*, 363−366.

Okumura, K., Inui, K., Hirai, Y., & Nakajima, T. (1981) *Biomed. Res. 2*, 450−452.

Pfeiffer, D. R., Gudz, T. I., Novgorodov, S. A., & Erdahl, W. L. (1995) *J. Biol. Chem. 270*, 4923−4932.

Roise, D., Horvath, S. J., Tomich, J. M., Richards, J. H., & Schatz, G. (1986) *EMBO J. 5*, 1327−1334.

Schwarz, G., & Robert, C. H. (1990) *Biophys. J. 58*, 577−583.

Schwarz, G., & Blochmann, U. (1993) *FEBS Lett. 318*, 172−176.

Schwarz, G., & Arbuzova, A. (1995) *Biochim. Biophys. Acta 1239*, 51−57.

Tanimura, A., Matsumoto, Y., & Tojyo, Y. (1991) *Biochem. Biophys. Res. Commun. 177*, 802−808.

Wakamatsu, K., Higashijima, T., Fujino, M., Nakajima, T., & Miyazawa, T. (1983) *FEBS Lett. 162*, 123−126.

Wakamatsu, K., Okada, A., Miyazawa, T., Ohya, M., & Higashijima, T. (1992) *Biochemistry 31*, 5654−5660.

Weinstein, J. N., Ralston, E., Leserman, L. D., Klausner, R. D., Dragsten, P., Henkart, P., & Blumenthal, R. (1984) in *Liposome Technology* (Gregoriadis, G., Ed.) pp 183−204, CRC Press, Boca Raton, FL.

Wolber, P. K., & Hudson, B. S. (1979) *Biophys. J. 28*, 197−210.

BI960342A